

## Surface shear stress, strain, and shear displacement for screw dislocations in a vertical slab with shear modulus contrast

Stuart McHugh and Malcolm Johnston *US Geological Survey,  
Menlo Park, California 94025, USA*

Received 1976 October 27; in original form 1976 June 18

**Summary.** Shear stresses, strains, and shear displacements on the free surface of a three-phase half-space (i.e. a half-space containing a vertical slab) produced by screw dislocations within the slab have been determined for shear modulus ratios in the range  $0.10 \leq \mu_{\text{slab}}/\mu_{\text{half-space}} \leq 10.0$  and depths of 1.0–10 km. Normalized quantities were computed using the ratios of stress, strain, or displacement in the three-phase material to those which would exist in a homogeneous medium. For modulus ratios less than 1.0, increasing the burial depth of the dislocation increases the normalized quantities, and the quantities decrease with increasing dislocation depth for modulus ratios greater than 1.0. With a modulus contrast of 0.25, which may be representative of parts of the San Andreas fault zone, and a single dislocation in the slab, increasing the dislocation depth from 1.0 to 10.0 km increases the normalized stress maximum from 0.45 to 0.95 and the normalized strain maximum from 1.7 to 3.8 in the slab. Normalized displacements are significantly different from 1.0 only within 1–2 fault-zone thicknesses of the dislocation. As the modulus ratio is changed from 1.0 to 0.25, and with only a single dislocation in the slab, the fraction of the displacement occurring within the fault zone to total displacement nearly doubles. A slip zone in the slab of finite width, modelled using a pair of dislocations with opposing Burger's vectors, causes the normalized quantities to decrease as the distance between the dislocations decreases.

### Introduction

Stresses, strains, tilts, and displacements for particular fault geometries are usually determined using the assumption that the medium is homogeneous (Chinnery 1961; Haskell 1969; Press 1965). However, significant variation in material properties, such as bulk and shear moduli, probably exist in these regions. The effect of these variations becomes quite important when measurements of stress, displacement, or displacement gradients are made near faults or other regions where a contrast in material properties occurs. The effect of a cavity is an extreme example (Harrison 1976).

The effect of horizontal and oblique layering on strains and displacements has been investigated by Rybicki (1971), Sato (1974), and Sato & Yamashita (1975), but the effect of vertical discontinuities on material properties has generally been neglected. Rybicki (1971) considered the case of two abutting quarter spaces with differing shear moduli but did not evaluate the effect of a vertical discontinuity in shear modulus on stresses, strains, or displacements. Chou (1966) used the method of images to determine the shear stresses existing in an infinite elastic three-phase material (i.e. two half-spaces separated by a vertical slab) for a screw dislocation either in the slab or one of the half-spaces.

This paper uses Chou's solution, for the stresses associated with a single dislocation in a vertical slab, modified to include the effect of a free surface by superposing a mirror dislocation. The shear stress, strain, and shear displacement existing at the free surface are computed for variations in the depth of the single dislocation and the shear modulus ratio. The effect of a slip zone of finite width on the normalized surface quantities was determined for variable modulus ratios and slip zone widths using a pair of screw dislocations with opposing Burger's vectors.

### Results for a single dislocation

The coordinate system used for the semi-infinite, elastic, three-phase material is shown in Fig. 1. The  $y$ , or vertical, axis forms one of the boundaries of the slab; the free surface is introduced at  $y = 0.0$ . In order to illustrate the effect of modulus contrast and dislocation depth, a particular case is considered where the slab thickness and the Burger's vector of the screw dislocation are held constant (1.0 km and 1.0 mm respectively); and  $\mu_3$  is set equal to  $\mu_1$ . Increasing the slab thickness will increase the half-width of the  $xz$  stress profile within the slab, and increasing the Burger's vector will increase the  $xz$  stress amplitude proportionally (similarly for the strains and displacements).

Although it is not certain what modulus ratio is appropriate for the San Andreas fault zone, analysis of tilt and strain observations suggests that the shear modulus within the fault zone may be at least an order of magnitude less than in the surrounding material (Alewine & Heaton 1973; Wood, Allen & Allen 1973; King, Nason & Burford 1976).

To model the variations in shear stress, strain, and shear displacement that may occur across the San Andreas fault in central California, the shear modulus within the slab ( $\mu_2$ ) was varied from  $3.0 \times 10^{10}$  dynes/cm<sup>2</sup> to  $3.0 \times 10^{12}$  dynes/cm<sup>2</sup>; and one of the values chosen for display was  $\mu_2 = 0.75 \times 10^{11}$  dynes/cm<sup>2</sup>\*. The quarter-space modulus ( $\mu_1$ ) was assumed

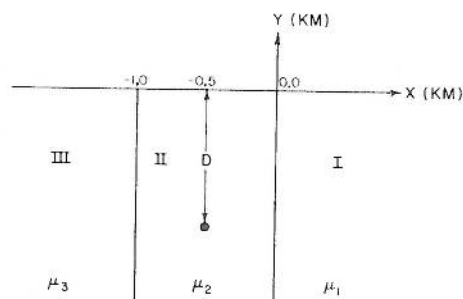


Figure 1. Screw dislocation embedded in centre of vertical slab at depth  $D$ . Burger's vector is positive into the page. The shear moduli in phases I, II, and III are  $\mu_1$ ,  $\mu_2$ , and  $\mu_3$  respectively.

\* Bakun & Bufe (1975) report shear-wave ( $S_3$ ) velocities in the fault zone of about 1.6 km/s, or about half their velocity in the surrounding material. This suggests a shear modulus contrast between the two regions of about 0.25.

to be  $3.0 \times 10^{11}$  dynes/cm<sup>2</sup>, and depths to the screw dislocation of 1.0, 5.0, and 10 km were used. All quantities were computed at the free surface, and normalized values were determined by taking ratios of the calculated shear stress, strain, or shear displacement in the three-phase material to the same quantities in the homogeneous half-space ( $\mu_1 = \mu_2 = \mu_3 = 3.0 \times 10^{11}$  dynes/cm<sup>2</sup>).

Increasing the dislocation depth ( $D$ ) reduces the amplitude of the free surface shear stresses ( $\sigma_{xz}^s$ ) and strains ( $e_{xz}^s$ ). If  $D$  is constant, increasing  $\mu^*$  (the shear modulus ratio is defined as  $\mu^* = \mu_2/\mu_1$ ) will increase  $\sigma_{xz}^s$  and decrease  $e_{xz}^s$ . The displacement ( $w^s$ ) across the fault zone increases if  $\mu^*$  decreases and the dislocation depth is held constant. Fig. 2(a), (b) and (c) display the effect of modulus ratio on the normalized shear stress ( $\sigma_{xz}^0$ ), strain ( $e_{xz}^0$ ), and shear displacement ( $w^0$ ) for a dislocation buried at 1.0 km and  $\mu^* = 0.10, 0.25$ , and 10. Figs 3 and 4 display the effect of dislocation depth on  $\sigma_{xz}^0$ ,  $e_{xz}^0$ , and  $w^0$  for  $\mu^* = 0.10$  and 0.25, respectively. Fig. 5 summarizes the effect of modulus ratio and dislocation depth on  $\sigma_{xz}^0$  and  $e_{xz}^0$  at a point on the surface directly above the dislocation.

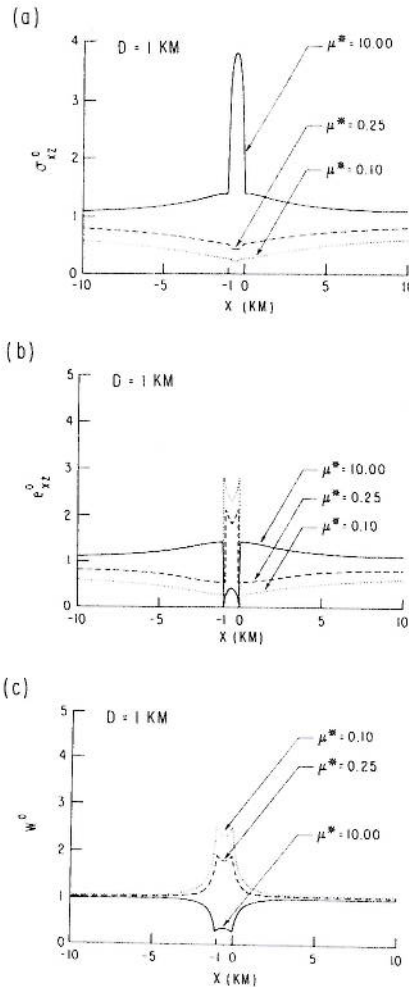


Figure 2. (a) Normalized surface shear stress,  $\sigma_{xz}^0$ , (b) normalized surface shear strain,  $e_{xz}^0$ , and (c) normalized surface displacements  $w^0$ , computed from  $e_{xz}^s$ , for a dislocation at a depth of 1.0 km and shear modulus contrasts ( $\mu^*$ ) of 0.10, 0.25, and 10.0.

**Modulus contrast effects for a single dislocation**

For a dislocation depth of 1.0 km as the shear modulus ratio between the slab and the surrounding material ( $\mu^*$ ) is increased from 0.10 to 10.0, the stress maximum ( $\sigma_{xz}^s$ ) increases by more than an order of magnitude (from  $1.1 \times 10^4$  dynes/cm<sup>2</sup> to  $1.8 \times 10^5$  dynes/cm<sup>2</sup>), but the strain maximum ( $e_{xz}^s$ ) above the dislocation ( $x = -0.5$  km) decreases by a factor of 6.0 (from  $0.37 \times 10^{-6}$  to  $0.06 \times 10^{-6}$ ). As  $\mu^*$  increases, the half-width of both stress and strain profiles increases, i.e. a decreasing modulus in the slab acts to confine the stress and strain within the slab. Although the total displacement is only slightly affected by  $\mu^*$ , the fraction of the displacement occurring within the slab when  $\mu^* = 1.0$  is about 3.0 times greater than that when  $\mu^* = 10$ , for a burial depth of 1.0 km.

Fig. 2 displays the variation with distance of the normalized quantities for a dislocation depth of 1.0 km. At distances from the dislocation greater than one or two fault-zone thicknesses,  $\sigma_{xz}^0$ ,  $e_{xz}^0$ , and  $w^0$  approach 1.0 slowly. At large distances, increasing  $\mu^*$  causes  $\sigma_{xz}^0$  and  $e_{xz}^0$  at a specific distance to approach 1.0. Above the dislocation ( $x = -0.5$  km),  $\sigma_{xz}^0$

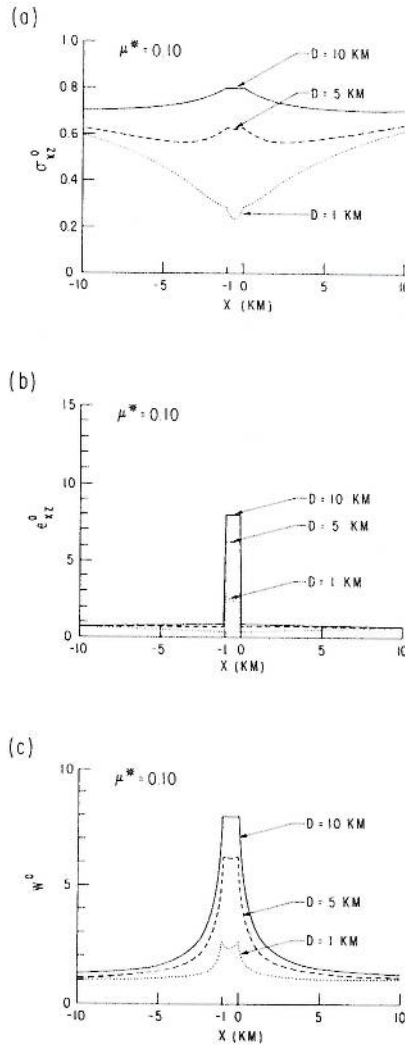


Figure 3. (a)  $\sigma_{xz}^0$ , (b)  $e_{xz}^0$ , and (c)  $w^0$  for  $\mu^* = 0.10$  and  $D = 1.0, 5.0,$  and  $10.0$  km.

and  $e_{xz}^0$  (Fig. 2(a) and (b)) are about 4 and 0.4 respectively when  $\mu^* = 10.0$  but become 0.5 and 1.8 respectively when  $\mu^*$  is 0.25, and 0.20 and 2.5 when  $\mu^*$  is 0.10. The normalized displacements – Fig. 2(c) – show significant departure from 1.0 only within 1–2 fault-zone thicknesses of the dislocation. As  $\mu^*$  decreases, more displacement occurs within the fault zone. When  $\mu^* = 0.25$ , the displacement across the fault zone ( $w_{fz}^s$ ) is nearly double that found when  $\mu^* = 1.0$ , and at  $\mu^* = 0.10$ ,  $w_{fz}^s$  is 2.4 times greater than at  $\mu^* = 1.0$ .

**Depths effects for a single dislocation**

Figs 3, 4 and 5 display the behaviour of  $\sigma_{xz}^0$ ,  $e_{xz}^0$ , and  $w^0$  as the dislocation depth ( $D$ ) is varied. With  $\mu^*$  less than 1.0,  $\sigma_{xz}^0$  approaches 1.0 as  $D$  is increased; however,  $e_{xz}^0$  within the fault zone is much greater than 1.0. At  $\mu^* = 0.10$ ,  $e_{xz}^0$  triples for an order of magnitude increase in  $D$  (at a point on the surface above the dislocation), and at  $\mu^* = 0.25$ ,  $e_{xz}^0$  doubles

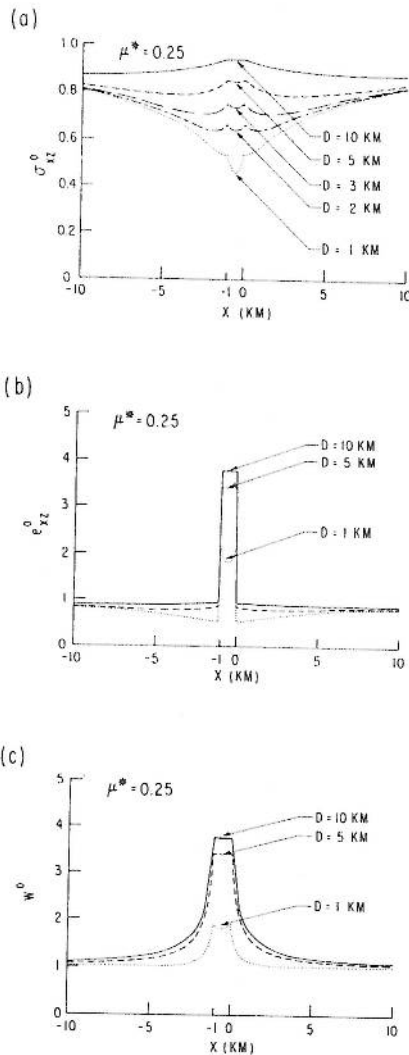


Figure 4. (a)  $\sigma_{xz}^0$ , (b)  $e_{xz}^0$ , and (c)  $w^0$  for  $\mu^* = 0.25$ ;  $D = 1.0, 2.0, 3.0, 5.0$  and  $10.0$  km – Fig. 4(a) – and  $D = 1.0, 5.0$ , and  $10.0$  km – Fig. 4(b) and (c).

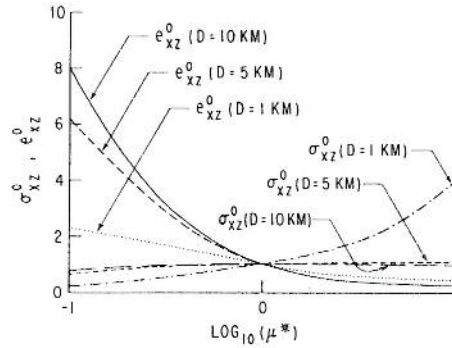


Figure 5.  $\sigma_{xz}^0$ , and  $e_{xz}^0$ , computed at  $x = -0.5$  km, against  $\mu^*$  for  $D = 1.0, 5.0$ , and  $10.0$  km.

when  $D$  is increased an order of magnitude. With  $\mu^* = 10.0$ ,  $\sigma_{xz}^0$  in the fault zone quadruples with an order of magnitude decrease in  $D$ , but  $e_{xz}^0$  in the fault zone is nearly constant as  $D$  is varied. Significant changes in  $w^0$  in the fault zone as  $D$  varies occur only when  $\mu^* < 1.0$ , and the variations in  $w^0$  follow the same pattern as the variation in  $e_{xz}^0$ .

#### Summary for a single dislocation

The changes in  $\sigma_{xz}^0$  and  $e_{xz}^0$  at  $x = -0.5$  km, for the range of variations in  $\mu^*$  and  $D$  are summarized in Fig. 5. Stresses caused by shallow dislocations ( $D \sim 1.0$  km) are affected by variations in  $\mu^*$  more than those caused by deep dislocations ( $D = 5.0$ – $10.0$  km). Decreasing  $\mu^*$  from 1.0 to 0.10 causes  $\sigma_{xz}^0$  to decrease from 1.0 to 0.20 for a depth of 1.0 km, but causes a decrease from 1.0 to 0.80 for a depth of 10.0 km. Increasing  $\mu^*$  from 1.0 to 10.0 will increase  $\sigma_{xz}^0$  by a factor of 4.0 for  $D = 1.0$  km but not at all for  $D = 10.0$  km.

#### Results for a slip zone of finite width

The effects of a slip zone of finite width on the normalized surface quantities were determined using a pair of screw dislocations with opposing Burger's vectors separated by a distance  $W$ . The upper boundary of the zone is at a depth,  $D$ , and the lower boundary is at a depth,  $D + W$ . Fig. 6 summarizes the effect of a zone of variable width on  $e_{xz}^0$ . The Burger's vector of the upper and lower boundaries are fixed at  $+1.0$  mm and  $-1.0$  mm respectively. The slab extends from  $x = 0.0$  km to  $x = -1.0$  km, and the slip zone position is fixed at  $x = -0.5$  km. The depth of the upper boundary,  $D$ , is fixed at 1.0 km, and  $W = 1.0$  km—Fig. 6(a)—or 5.0 km—Fig. 6(b)—while  $\mu^*$  is varied. In Fig. 6(c),  $D = 1.0$  km,  $\mu^* = 0.25$  and  $W = 1.0, 5.0$ , and  $10.0$  km. The discontinuities in  $\sigma_{xz}^0$  and  $e_{xz}^0$  outside the fault zone are caused by zero crossings in the homogeneous half-space profiles.

Increasing the depth to the upper boundary,  $D$ , causes the non-normalized profiles,  $\sigma_{xz}^0$  and  $e_{xz}^0$ , to broaden and moves the discontinuities in  $\sigma_{xz}^0$  and  $e_{xz}^0$  further from the fault zone. The non-normalized displacements approach zero far from the dislocations consequently  $w^0$  is not displayed. Otherwise, the changes in  $\sigma_{xz}^0$  and  $e_{xz}^0$  for a dislocation pair produced by variations in  $D$  are analogous to the single dislocation case and will not be pursued further here. Increasing  $W$  also causes the profiles to broaden, although not so much as increases in  $D$ . At any given position,  $x$ , the effect of an increase in  $W$  is to increase  $\sigma_{xz}^0$  and  $e_{xz}^0$ . In the limit, with  $W$  very large,  $\sigma_{xz}^0$ ,  $e_{xz}^0$ , and  $w^0$  will appear to be produced by a single dislocation.

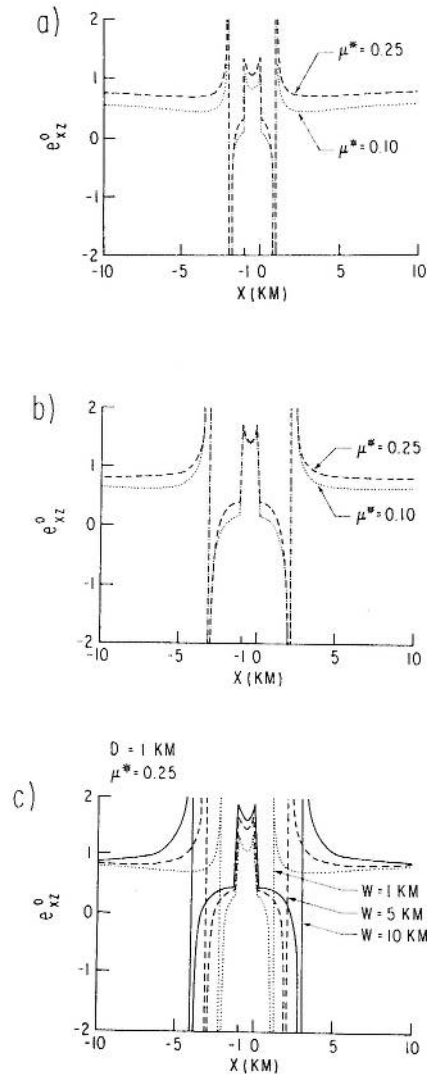


Figure 6. Effect of a slip zone of finite width (at a position  $x = -0.5$  km),  $W$ , and of variable modulus ratio,  $\mu^*$ , on the normalized surface shear strain  $e_{xz}^0$ . The upper boundary of the slip zone,  $D$ , is fixed at 1.0 km; the lower boundary is at a depth,  $D + W$ . (a)  $e_{xz}^0$  for  $W = 1.0$  km and  $\mu^* = 0.10$  and 0.25, (b)  $e_{xz}^0$  for  $W = 5.0$  km and  $\mu^* = 0.10$  and 0.25, (c)  $e_{xz}^0$  for  $\mu^* = 0.25$  and  $W = 1.0, 5.0$  and 10.0 km.

#### Data

In addition to the coseismic and tidal data cited previously that suggest the occurrence of variations in shear modulus across the fault zone, there is also some evidence for these variations from observations of creep-related tilt events. Analysis of creepmeter and tiltmeter data from the Melendy Ranch and Bear Valley sites, approximately 30 km south of Hollister, California, indicates a slight discrepancy between predicted and observed amplitudes of creep-related tilt events (McHugh & Johnston 1976). Amplification caused by non-uniform material properties may result in an overestimate of the amount of slip required to produce the signal and a disagreement in the displacement and displacement gradients between predictions based on a half-space model and observations made in a vertically

layered material. If the tilt amplitudes are affected by a modulus contrast in a manner analogous to the strain amplitudes, tilts at points within the fault zone will be enhanced when  $\mu^* < 1.0$ , which may explain the absence of observable creep-related tilt signals at Bear Valley. Measurements made of the strain and tilt field across the fault zone may be expected to provide information about any contrast in material properties between the fault zone and surrounding medium.

### Conclusions

Although variations in shear modulus of many orders of magnitude may be unlikely along the San Andreas fault zone, a modulus contrast of 0.10–0.25 may occur. If  $\mu^* = 0.10$ , the strains may be amplified by a factor of 2–8, and if  $\mu^* = 0.25$ , strains 50–150 per cent larger than those predicted for a homogeneous material can occur for slip at depths of 1.0–10.0 km. If sections of the fault zone are even less rigid ( $\mu^* < 0.10$ –0.25), strain measured in the fault zone at the surface will greatly overestimate the slip at depth. For points outside the fault zone and  $0.10 < \mu^* < 10.0$  the strains will be nearly equal to those expected for a homogeneous material.

### Acknowledgment

We thank Dr K. Rybicki and Professor K. Kasahara for a preprint of their work on faulting in an inhomogeneous medium.

### References

- Alewine, R. W. & Heaton, T. H., 1973. Tilts associated with the Pt. Mugu earthquake, Proc. Conf., Tectonic problems of the San Andreas fault system, *Stanford Univ. Publ., Geol. Sci.*, XIII, 94–103.
- Bakun, W. H. & Bufe, C. G., 1975. Shear wave attenuation along the San Andreas fault zone in central California, *Bull. seism. Soc. Am.*, 65, 439–459.
- Chinnery, M. A., 1961. The deformation of the ground around surface faults, *Bull. seism. Soc. Am.*, 51, 355–372.
- Chou, Y. T., 1966. Screw dislocations in and near lamellar inclusions, *Phys. Stat. Sol.*, 17, 509–516.
- Harrison, J. C., 1976. Cavity and topographic effects in tilt and strain measurements, *J. geophys. Res.*, 81, 319–328.
- Haskell, N. A., 1969. Elastic displacements in the near-field of a propagating fault, *Bull. seism. Soc. Am.*, 59, 865–908.
- King, Chi-Yu, Nason, R. D. & Burford, R. O., 1976. Coseismic steps recorded on creepmeters along the San Andreas fault, *J. geophys. Res.*, in press.
- McHugh, S. & Johnston, M., 1976. Some short period nonseismic tilt perturbations and their relation to episodic slip on the San Andreas fault, *J. geophys. Res.*, 81, 6341–6346.
- Press, F., 1965. Displacements, strains, and tilts at teleseismic distances, *J. geophys. Res.*, 70, 2395–2412.
- Rybicki, K., 1971. The elastic field of a very long strike-slip fault in the presence of a discontinuity, *Bull. seism. Soc. Am.*, 61, 79–92.
- Sato, R., 1974. Static deformations in an obliquely layered medium, part I. Strike-slip fault, *J. Phys. Earth*, 22, 455–462.
- Sato, R. & Yamashita, T., 1975. Static deformation in an obliquely layered medium, part II. Dip slip fault, *J. Phys. Earth*, 23, 113–126.
- Wood, M. D., Allen, R. V. & Allen, S. S., 1973. Methods for prediction and evaluation of tidal tilt data from borehole and observatory sites near active faults, *Phil. Trans. R. Soc. Lond. A.*, 274, 245–252.